PSEUDOMORPHS OF KAOLINITE AFTER BIOTITE
(STUDIES ON MECHANISM OF WEATHERING, 1 ST REPORT.)

By

Takeshi MITSUDA

(With 3 Plates, 2 Tables and 6 Figures)
Contributions from the Department of Geology and Mineralogy
Faculty of Science, Hokkaido University, No 798

CONTENTS

Abstract

The writer found specimens of pseudomorphs of kaolinite after biotite from deep-weathered granite. X-ray analyses indicate that the specimens are highly-crystalline kaolinite with the basal spacing of 7.17 Å and that the c-axis is closely similar in direction to that of biotite before kaolinite. As for the chemical composition, the ratio of Al to Si is 0.89~1.07 for all individual particles analysed.

From the geological point of view, the granite in Seto district, northern part of Nagoya City, has been bathed for a long period in percolating ground water with pH values from 5 to 6, common pH values of ground water rich in CO_2 and organic acids. In this pH region, the solubility of Al_2O_3 derived from biotite may be neglected, since it is very small compared to other elements entering into the compositions of biotite.

On the assumption that Al has remained constant from biotite to kaolinite, it is noteworthy that the weathering process is the requirement for a large amount of volume change which may be calculated theoretically. In fact, the volume of kaolinite after biotite is very small compared with unaltered biotite from the same granite.

It is pointed out that the shrinkage was involved mainly within the cleavage plane.

Introduction

Many investigators such as geologists, mineralogists, chemists, and soil scientists, have provided a tremendous amount of information on the mechanism of weathering. However they have not always agreed on the step-by-step mechanism by which one mineral is weathered or altered to another.[1)]

From the chemical point of view, the main factors controlling the weathering process may be summarized as follows:

The pH of solution, composition and crystallinity such as glassy or crystalline state of parent materials, and oxidation-reduction potentials of environment must be considered.

Regarding only the factors mentioned above, we could not gain any information about how and why some clay minerals concentrate in some districts and some geological ages. This is very important problems of geology and mineralogy. Hence, fundamentally, geochemical studies should yield information about step-by-step weathering mechanism.

Biotite and feldspar are important constituents of many igneous rocks and of some metamorphic rocks such as gneiss and schist. It has long been known by the geologists and mineralogists that certain crystalline minerals show evidence of the existence of pseudomorphs such as kaolinite after mica, chlorite after biotite, kaolinite or halloysite after feldspar, bastite after hypersthene, hematite after magnetite, limonite after pyrite and numerous others.

It is obvious that the examination of the pseudomorphs discussed here will yield information on the nature of one weathering mechanism directly related to biotite and deep-weathering mechanism of granite.

Earlier investigation of pseudomorphs of kaolinite after biotite was made by TAKAYASU[2)] in 1950, and recently Roy et al. have reported *WEATHERING STUDIES.*[3) 4)]

Mode of occurrence and crystal habit

There are many kaolin deposits in Seto district, northern part of Nagoya City, Japan. They were transported mainly from deep-weathered granite which is a basal rock in this district. Kaolin bedding is rhythmically interbedded with silicious sand which is composed of quartz from granite.

The genesis of the kaolin clay deposits of Seto district is inferred in Fig. 1 and will be discussed following paper.

The kaolinite after biotite considered here was collected in deep-weathered granite which is preserved granitic texture.

Th specimens are yellow to yellowish brown in color, less than about 1×1×2 mm. in size and take the form mainly of hexagonal prisms such as biotite as shown in Plate I, some of which show long prisms curvatured along to c-axis.* The average volume and weight measured for 300 particles are 0.647 mm^3 and 1.60 mg per one particle.

In thin section, it is noteworthy that cleavages of the specimens run mainly parallel with each other, through detailed observation shows that

Fig. 1. Provenance of kaolin deposits in Seto district.

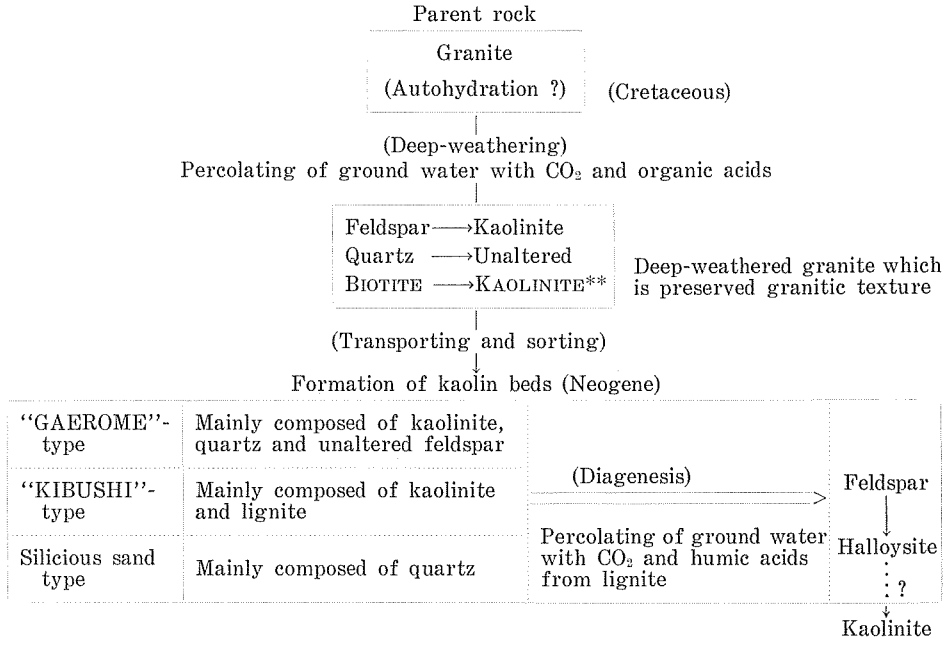

* Specimens are very similar in appearance to kaolinite books from the Georgia clay deposits.[15]

** Specimens considered here.

direction of cleavage is not linear, but slightly zigzag as shown in Plate II. This is very important evidence for considering mechanism of weathering from biotite to kaolinite and will be discussed later. Sometimes, as shown in Plate II, B, the specimen shows brownish part of less pleochroism. It is a disordered biotite parallel with cleavage planes.

It is not indicated by X-ray studies that the specimens have a mixed-layered lattice between kaolinite and biotite.

Experimental

X-ray analyses

The X-ray powder patterns of the specimens were obtained by a Philips Geiger Counter X-ray Spectrometer with filtered Cu kα radiation. The experimental conditions were as follows:

35 Kv., 13 mA., scale factor 4, multiplier 1.0, time constant 4 seconds, scaning speed 2° or 1° per minute, angular aperture 1°, receiving slight 0.006 inch.

The X-ray powder diffraction patterns of the specimens are depicted in Fig. 2 and their spacings are given in Table 1.

The results are summarized as follows:

(1) It is clear that the specimens after biotite are composed mainly of kaolinite with a basal spacing reflection of 7.17 Å (001), which is of slightly disordered type as revealed by unification of the close doublets $(11\bar{1})$ and $(1\bar{1}\bar{1})$.

TABLE 1. X-ray diffraction data.

*hkl**	*d*	I
B	10.0	4*b*
001	7.17	160
020	4.44	15*b*
002	3.578	110
$20\bar{1}$, $1\bar{3}0$, 130	2.561	10*b*
$13\bar{1}$, 112, 200	2.499	10*b*
003	2.380	15*b*
$20\bar{2}$, $1\bar{3}1$, $11\bar{3}$	2.339	15*b*
$20\bar{3}$, $1\bar{3}2$	1.997	5
004	1.790	5
$24\bar{0}$, $20\bar{4}$, $1\bar{3}3$	1.666	5*b*
060, $33\bar{1}$, $33\bar{1}$	1.486	5

b: broad lines, *B*: biotite, *: indices after BRINDLEY[10]

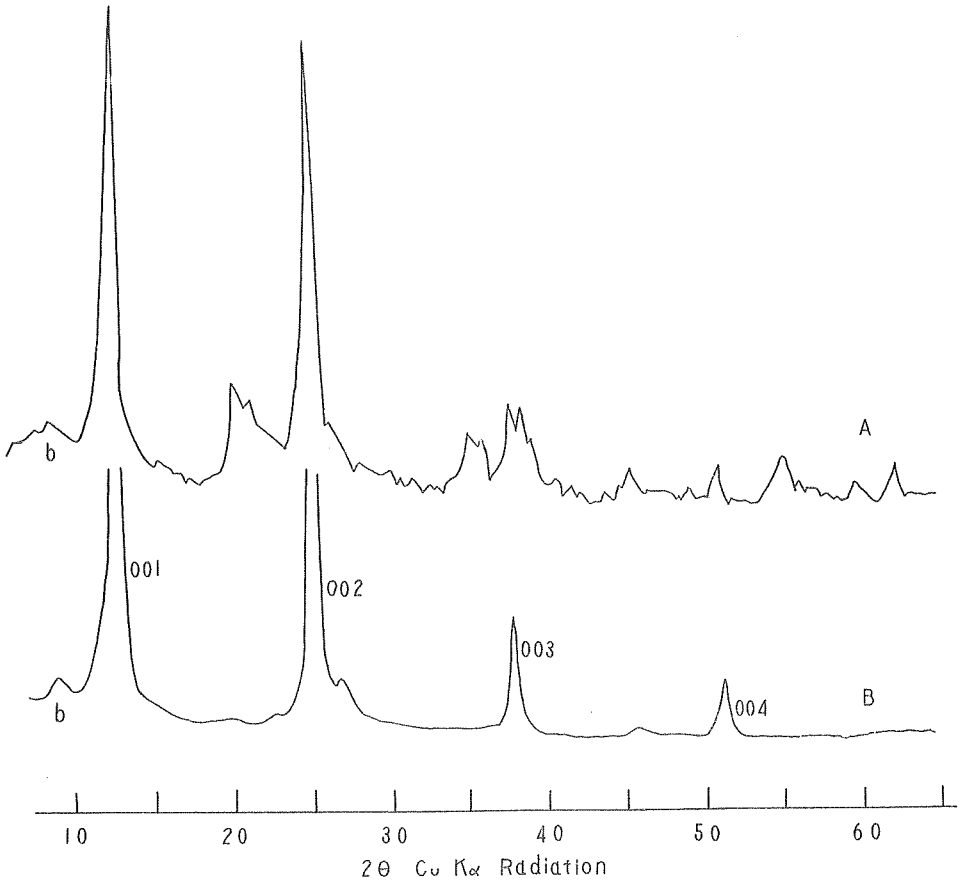

Fig. 2. X-ray diffraction patterns.
A: powder specimens, B: oriented specimens

(2) A weak and broad line of 10 Å approximates to the reflection of biotite (001) which is a disordered one.

(3) The oriented layered specimens parallel with cleavage plane surfaces as shown in Fig. 2, B, give a clear sequence of four basal reflections viz., (001), (002), (003) and (004) from the 7.17 Å basal spacing, and a weak and broad line of 10.0 Å.

Those results indicate that the c-axes between kaolinite after biotite and biotite before kaolinite are closely similar in their directions.

Differential thermal analysis curve

Heating rate for differential thermal analysis was 10°C per minute.

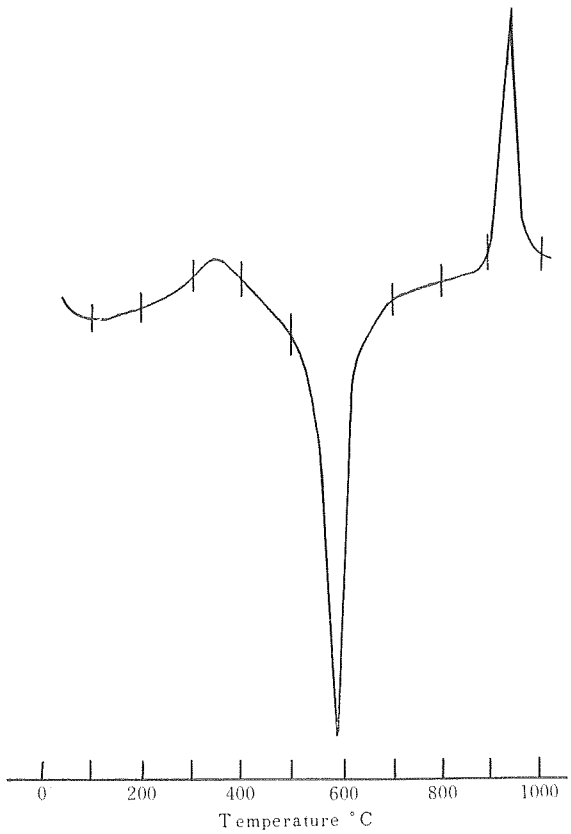

Fig. 3. Differential thermal analysis curve.

The differential thermal analysis curve of the specimens as shown in Fig. 3, displays the following peaks:

(1) A weak endothermic peak in the temperature range of 100°~200°C, and a sharp one in 595°C.

(2) A weak exothermic peak in the range of 300°~400°C and a sharp one in 950°C.

Those peaks prove that the specimens are mainly composed of highly-crystalline kaolinite as indicated in X-ray diffraction patterns. The first weak endothermic peak at below 200°C represents the loss of adsorbed water from cleavage plane surfaces.

Dehydration curve

The heating rate for dehydration analysis was 10°C per minute.

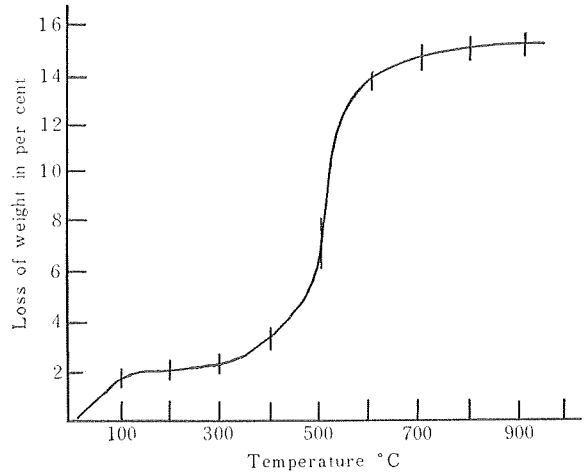

Fig. 4. Dehydration curve.

The dehydration curve of the specimens, as in Fig. 4, shows that at temperature below 100°C there is rapid loss of small amounts of water and a very slight loss up to 400°C. From 500° to 600°C the hydroxyl water is lost rapidly and abruptly. Above 600°C there is again a gradual loss of water up to about 800°C, where dehydration is essentially complete. Those peaks for dehydration are very similar to those of differential thermal reactions.

Infrared absorption spectra

Infrared absorption spectra were recorded on a HILGER H. 800 using sodium chlorite optics in the region 4000 to 650 Cm^{-1}. The samples taken 20 mg in amout after and before heating were prepared and exposed as mulls of uniform thickness by using 0.07 cc Nujol. Infrared spectra of the specimens before heating and after heating up to 110°C, as shown in Fig. 5 correspond closely with patterns of the reference kaolinite.

As for the pattern of C after heating up to 600°C, the absence of a sharp band at about 3660 Cm^{-1} shows that in this temperature, kaolinite dehydrates as indicated by the differential thermal analysis and dehydration curve.

Chemical composition

The chemical composition, ratio of Si to Al or Fe, was determined by colorimetrically[5] for individual particles as given below:

	Al/Si	Fe/Si (Analyst: K. GOTO)
A	1.00	0.037
B	1.00	0.065
C	1.02	0.047
D	1.07	0.054
E	0.89	0.129

These results show that the ratio of Al to Si for particles A to D are very similar to the theoretical value of kaolinite and for particle E which is slightly lowest in that ratio, highest in ratio Fe to Si among them. It might be expected that particle E has an unaltered part of biotite as shown in Plate II, B.

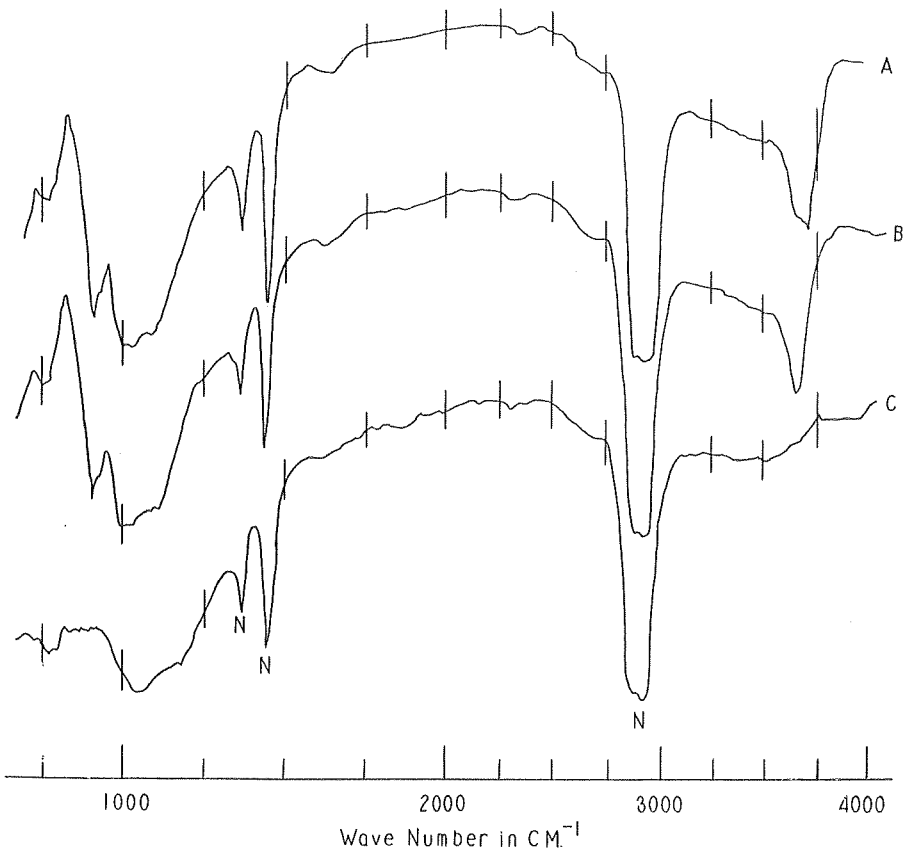

Fig. 5. Infrared absorption curves.
A, before heating B, heating for 2 hours at 110°C
C, heating for 2 hours at 600°C N, absorption by Nujol

Specific gravity, volume and porosity

Average apparent specific gravity and volume were determined for 300 particles as given below:

$$\text{Sp. G.} = 2.475\left(\frac{18^{\circ}C}{4^{\circ}C}\right), \qquad \text{Volume} = 0.647\ \text{mm}^3$$

The apparent specific gravity is slightly lower than the theoretical value of 2.618 computed from the structure after BRINDLEY.[10] This datum would probably indicate the presence of closed pores in the specimens. If so, the porosity of the specimens may be calculated as a value of about 5.5 per cent.

Discussion

Chemical factors controlling weathering process

The granite in Seto district has been bathed for a long period in percolating ground water with pH values from 5 to 6, common pH values of ground water rich in CO_2 and organic acids, especially humic acids.

In this pH region, alkali metals in interlayer positions are first soluble and first moved away from lattices.

CORRENS[6] pointed out that at pH values from 5 to 9, Al_2O_3 is very slightly soluble whilst SiO_2 become more and more soluble. At pH 10 and higher, Al_2O_3 and SiO_2 are both soluble. Therefore, at low pH values SiO_2 is insoluble and Al_2O_3 is soluble.

OKAMOTO, OKURA and GOTO,[7] and GOTO, OCHI and OKURA[8] have shown that the solubility of amorphous silica increases rapidly with temperature and pH. Therefore, the solubility of aluminum at pH values below 5 or above 9 is abruptly increased but negligible at pH values from 5 to 9.

The general attributes of solubility for aluminum silicate minerals are not well known, but the data given by CORRENS and by OKAMOTO and his colleagues for solubility of amorphous materials strongly indicate that aluminum in silicate minerals is also very insoluble at the pH values of ground water considered here.

While silicon is being released from lattice of biotite, coordination of aluminum will be changed from four to six and Al-Si layered lattices will be repolymerized. That process cause a significant loss of volume to biotite.

Volume change

On the assumption that aluminum has remained constant from biotite to kalinite, it is noteworthy that the happening of the weathering process is the requirement for a large amount of volume change.

By determining the population of aluminum in a unit cell of biotite and its volume, the ratio of volume change from biotite to kaolinite may be calculated as below and as shown in Fig. 6.

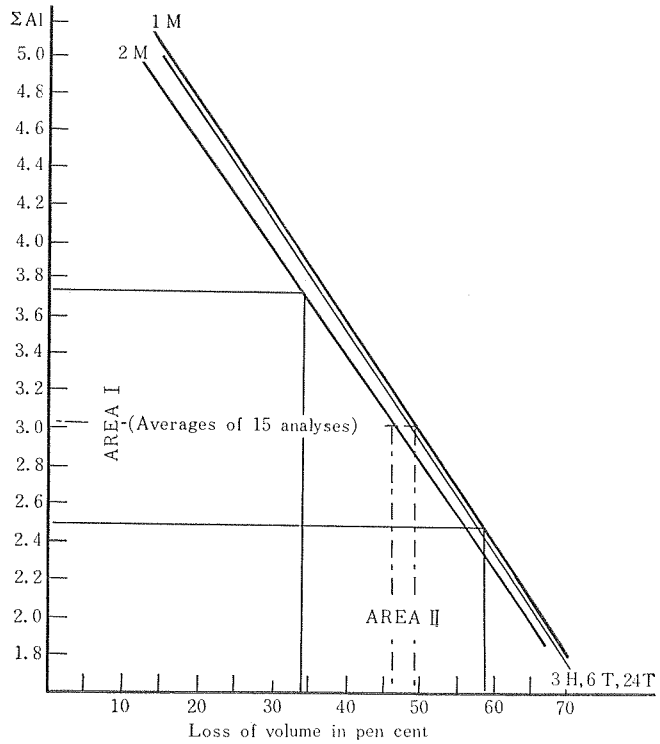

Fig. 6. Loss by volume change from biotite to kaolinite.

Biotite

$(K\ Na\ Ca)_2(R\ Al)_6(Al\ Si)_8O_{20}(OH \cdot F)_4$

R: Fe^{+2}, Fe^{+3}, Mg, Ti, Mn, Li

Chemical unit volume on the basis of $O_{20}(OH \cdot F)_4$

1 M —— 488.21 Å^3

2 M —— 465.85 Å^3

3 H, 6 T, 24 T —— 486.53 Å^3

Kaolinite

$Al_4Si_4O_{10}(OH)_8$

Chemical unit volume on the basis of $O_{10}(OH)_8$

327.32 Å^3

In the above, unit cell volumes are calculated from HENDRICKS' structure[9] for biotite and from BRINDLEY's structure[10] for kaolinite. According to many investigators, there are many cases of polytypism of micas, though volume on the basis of $O_{20}(OH{\cdot}F)_4$ per unit layer shows slight variation among structures in respect to polytypism.

$$\text{V. L. } (1\,\text{M}) = 100 - 16.76\,\Sigma\,\text{Al}$$
$$\text{V. L. } (2\,\text{M}) = 100 - 17.57\,\Sigma\,\text{Al}$$
$$\text{V. L. } (3\,\text{H},\ 6\,\text{T},\ 24\,\text{T}) = 100 - 16.82\,\Sigma\,\text{Al}$$

In the above, V.L. is loss of volume in per cent from biotite to kaolinite and Σ Al is the total of aluminum per chemical unit for biotite.

It is impossible to show strictly the chemical compositions of biotite

TABLE 2. Ionic formulae for some biotites.

ΣAl	K	Na	Ca	Σ	Si	Al	ΣIV	Al	Fe^{+2}	Fe^{+3}	Mg	Ti	Mn	Li	ΣVI	Oc.*	Ref.
3.69	1.40	0.32	0.41	2.13	5.50	2.50	8.00	1.19	2.58	0.42	0.08	0.02	0.08	0.16	4.53		11-2
2.52	1.73	0.17	0.05	1.95	5.60	2.40	8.00	0.12	1.93	0.52	2.71	0.38	0.07	—	5.73		11-6
2.85	1.66	0.12	0.10	1.88	5.43	2.57	8.00	0.28	2.63	0.21	2.02	0.43	0.04	—	5.61		11-10
3.76	1.97	0.11	0.04	2.12	5.62	2.38	8.00	1.38	3.93	0.09	0.10	0.40	0.06	—	5.96		12-8
3.57	1.72	0.11	0.00	1.83	5.32	2.68	8.00	0.89	2.13	0.08	2.20	0.30	0.04	—	5.64		12-12
2.68	1.62	0.12	0.10	1.84	5.56	2.44	8.00	0.24	2.43	0.12	2.52	0.38	0.02	—	5.71		12-13
2.78	1.67	0.15	0.07	1.89	5.35	2.65	8.00	0.13	3.44	0.36	1.42	0.33	0.11	—	5.79		12-15
2.54	1.75	0.08	0.06	1.89	5.62	2.38	8.00	0.16	0.96	0.10	4.58	0.10	0.01	—	5.91		12-16
2.67	1.73	0.13	0.10	1.96	5.50	2.50	8.00	0.17	3.56	0.25	1.18	0.40	0.07	—	5.63		12-17
3.19	1.48	0.15	0.14	1.77	5.32	2.68	8.00	0.51	3.38	0.29	1.05	0.27	0.22	—	5.72		12-18
3.22	1.46	0.08	0.19	1.73	5.59	2.41	8.00	0.81	2.73	0.97	0.07	0.18	0.12	0.15	5.03	from granite	13-11
2.60	1.51	0.52	0.13	2.16	5.39	2.60	7.99	0.00	3.54	0.40	1.15	0.35	0.18	—	5.62		14-4
2.91	1.19	0.50	0.09	1.78	5.28	2.72	8.00	0.19	2.85	1.44	0.43	0.28	0.11	—	5.30		14-9
3.09	0.98	0.38	0.35	1.71	5.13	2.87	8.00	0.22	3.01	1.38	0.38	0.24	0.12	—	5.35		14-10
3.16	1.29	0.37	0.25	1.91	5.31	2.69	8.00	0.47	2.86	1.17	0.35	0.24	0.12	—	5.21		14-11
3.02 [1]	1.54	0.22	0.14	1.90	5.43	2.57	8.00	0.45	2.80	0.52	1.35	0.29	0.09	0.02	5.52		
3.38	1.80	0.07	0.00	1.87	5.35	2.65	8.00	0.73	2.61	0.12	1.86	0.30	0.07	—	5.69		11-8
2.68	1.75	0.11	0.03	1.89	5.56	2.44	8.00	0.24	2.44	0.11	2.52	0.38	0.02	—	5.71		11-11
2.93	1.65	0.12	0.16	1.93	5.52	2.48	8.00	0.45	2.59	0.39	1.65	0.32	0.06	—	5.46		11-7
2.93	1.65	0.12	0.16	1.93	5.52	2.48	8.00	0.45	2.59	0.39	1.65	0.32	0.06	—	5.46		12-4
2.73	1.76	0.15	0.10	2.01	5.50	2.50	8.00	0.23	2.40	0.34	2.18	0.36	0.04	—	5.55		12-6
2.78	1.82	0.08	0.06	1.96	5.42	2.58	8.00	0.20	3.47	0.22	1.22	0.43	0.09	—	5.63		12-10
3.18	1.17	0.22	0.14	1.53	5.59	2.41	8.00	0.77	1.84	0.39	2.45	0.17	0.00	—	5.62	from migmatite and gneisose granite	14-1
3.25	1.55	0.24	0.12	1.91	5.40	2.60	8.00	0.65	1.90	0.24	2.61	0.22	0.00	—	5.62		14-3
2.98 [2]	1.64	0.14	0.10	1.88	5.48	2.52	8.00	0.46	2.48	0.28	2.02	0.30	0.04	—	5.58		

TABLE 2. Ionic formulae for some biotites. (*Continued*)

ΣAl	K	Na	Ca	Σ	Si	Al	ΣIV	Al	Fe^{+2}	Fe^{+3}	Mg	Ti	Mn	Li	ΣVI	Oc.*	Ref.
2.50	1.87	0.17	0.05	2.09	5.54	2.46	8.00	0.04	1.91	0.51	2.68	0.38	0.07	—	5.59	from diorite, granodiorite and gneisose diorite	12-1
3.38	1.80	0.07	0.00	1.87	5.35	2.65	8.00	0.73	2.61	0.12	1.86	0.29	0.07	—	5.68		12-3
2.85	1.83	0.08	0.06	1.97	5.43	2.57	8.00	0.28	2.42	0.34	2.36	0.38	0.05	—	5.83		12-5
2.85	1.66	0.12	0.10	1.88	5.43	2.57	8.00	0.28	2.63	0.21	2.02	0.43	0.04	—	5.61		12-14
2.76	1.80	0.05	0.06	1.91	5.46	2.54	8.00	0.22	3.67	0.13	1.30	0.45	0.08	—	5.85		12-19
2.59	1.73	0.09	0.02	1.84	5.49	2.51	8.00	0.08	2.32	0.09	2.67	0.53	0.03	—	5.72		12-21
3.18	1.77	0.10	0.04	1.91	5.35	2.65	8.00	0.53	2.67	0.10	1.84	0.41	0.08	—	5.63		12-21
3.26	1.81	0.10	0.02	1.93	5.34	2.66	8.00	0.60	2.67	0.08	1.82	0.37	0.10	—	5.64		12-22
2.92 [3]	1.78	0.10	0.04	1.92	5.42	2.58	8.00	0.34	2.62	0.20	2.07	0.41	0.07	—	5.71		
3.14	2.19	0.63	0.12	2.94	5.75	2.25	8.00	0.89	3.27	0.15	1.52	0.00	0.00	—	5.83	from pegmatite	11-3
3.26	2.10	0.52	0.12	2.74	5.68	2.32	8.00	0.94	3.29	0.62	0.10	0.00	0.15	—	5.10		11-4
3.03	1.55	0.18	0.01	1.74	5.23	2.77	8.00	0.26	2.71	1.57	0.29	0.10	0.15	0.16	5.24		13-1
3.04	1.38	0.11	0.15	1.64	5.35	2.65	8.00	0.39	3.27	1.45	0.03	0.07	0.16	0.03	5.40		13-2
2.67	1.53	0.04	0.13	1.70	4.89	2.67	7.56	0.00	3.00	2.62	0.11	0.01	0.05	0.09	5.88		13-3
2.53	1.31	0.16	0.05	1.52	5.40	2.53	7.93	0.00	2.04	2.39	0.22	0.17	0.14	0.06	5.02		13-4
3.82	1.58	0.41	0.14	2.13	5.33	2.67	8.00	1.15	0.86	2.52	0.50	0.17	0.12	0.06	5.38		13-8
5.10	1.49	0.01	0.18	1.68	4.98	3.02	8.00	2.08	1.14	1.12	0.43	0.03	0.07	0.05	4.92		13-9
4.53	1.45	0.30	0.15	1.90	4.93	3.07	8.00	1.46	1.53	1.35	0.46	0.03	0.07	0.09	4.99		13-10
2.70	1.52	0.13	0.06	1.71	5.66	2.34	8.00	0.36	3.68	0.90	0.14	0.09	0.10	0.16	5.43		13-12
3.83	0.98	0.20	0.10	1.28	4.91	3.09	8.00	0.74	2.44	1.21	1.26	0.10	0.03	—	5.78		14-7
3.98	1.46	0.23	0.07	1.76	5.27	2.73	8.00	1.25	1.52	1.53	0.48	0.12	0.05	—	4.95		14-8
3.22	1.26	0.70	0.20	2.16	5.33	2.67	8.00	0.55	2.69	1.30	0.19	0.19	0.12	—	5.04		14-12
3.45 [4]	1.52	0.28	0.11	1.91	5.29	2.68	7.97	0.77	2.42	1.44	0.44	0.08	0.09	0.05	5.29		
3.57	1.79	0.06	0.00	1.85	5.25	2.75	8.00	0.82	2.44	0.24	1.78	0.30	0.04	—	5.62	from gneiss and schist	11-9
3.57	1.79	0.06	0.00	1.85	5.25	2.75	8.00	0.82	2.44	0.24	1.78	0.30	0.04	—	5.62		12-2
3.50	1.85	0.12	0.00	1.97	5.33	2.67	8.00	0.83	2.30	0.08	1.99	0.34	0.04	—	5.58		12-9
3.00	1.86	0.08	0.02	1.96	5.41	2.59	8.00	0.41	2.72	0.10	2.00	0.38	0.06	—	5.67		12-11
3.49	1.72	0.13	0.00	1.85	5.32	2.68	8.00	0.81	2.45	0.03	1.76	0.46	0.02	—	5.53		12-23
3.94	1.22	0.35	0.10	1.67	5.10	2.90	8.00	1.04	1.85	0.19	2.27	0.30	0.00	—	5.65		14-2
3.31	1.20	0.24	0.01	1.45	5.44	2.56	8.00	0.75	1.73	1.01	2.04	0.04	0.05	—	5.62		14-5
3.40	1.69	0.29	0.02	2.00	5.58	2.42	8.00	0.98	2.12	0.40	1.92	0.32	0.01	—	5.75		14-6
3.47 [5]	1.64	0.17	0.02	1.83	5.34	2.66	8.00	0.81	2.26	0.29	1.94	0.31	0.03	—	5.64		
3.17 [6]	1.61	0.20	0.09	1.90	5.39	2.60	7.99	0.57	2.54	0.63	1.43	0.26	0.07	0.02	5.52		

[1] averages of 15 analyses [2] averages of 8 analyses [3] averages of 8 analyses
[4] averages of 13 analyses [5] averages of 8 analyses [6] averages of 52 analyses
* Occurrence

before kaolinite considered here, so only the probability is shown for loss of volume change by calculation of population of aluminum in biotite from many chemical data after HARADA[11),12),13),14)].

In the calculation from analyses, the structural formulae were constructed on the basis of (O+OH) or (O+OH·F)=24. The calculated data are given in Table 2, which show average values or varieties of populations of aluminum and other ions for biotites.

For example, AREA 1 in Fig. 6 shows range of aluminum populations for 15 analyses of biotites from granites and AREA II shows range of loss of volume in per cent for many polytypisms of biotite to kaolinite.

Evidence

The average volume of the specimens, kaolinite after biotite, and biotite from the same rock are determined for 300 particles as below:

Kaolinite after biotite —— 0.647 mm^3
Biotite —— 2.069 mm^3

Those data indicate that the loss of volume is about 69 per cent. This value is higher than the probability mentioned above since the X-ray diffraction patterns show that the specimens for biotite had altered to vermiculite.

It is impossible to show strictly the loss of volume for the specimens discussed here, but possible to point out that the shrinkage is connected mainly within the cleavage plane. Accordingly, in thin section the direction of cleavage for kaolinite after biotite is not linear but slightly zigzag whilst crystal habit shows long prism which is curvatured along to c-axis.

Finally electron micrograph is shown of cleavage plane surface from one of the specimens discussed above in Plate III. It seems certainly that the cleavage surface has many closed pores of about 0.1 micron in diameter as expected from the about 5.5 per cent porosity. This item will be discussed in a following paper.

Acknowledgments

The author is greatly indebted to Professor Zyunpèi HARADA, Hokkaido University, for reading this manuscript and offering significant suggestions on pseudomorph problems.

Thanks are due to Mr. K. GOTO, for chemical analyses, to Professor S. WATANABE, for the use of electron microscope and to Assistant Pro-

fessor S. MATSUSHITA, for infrared absorption analyses.

He is also indebted to Assistant Professors M. HUNAHASHI and S. SASAKI for suggestions on weathering problems of rocks and soils.

References

1) KELLER, W. D. (1957): The Principles of Chemical Weathering. Lucas Brothers Publishers, Columbia, Missouri.
2) TAKAYASU, M. (1950): On the Kaolinite Crystal From Numaushi, Hokkaido, Japan. (Preliminary Report) Jour. Fac. Sci. Hokkaido Univ., Ser. IV, Vol. VII, Nos. 3, pp. 315–318.
3) ROY, R., and L. A. ROMO (1957): Weathering Studies. 1. New Data on Vermiculite. Jour. Geology, Vol. 65, pp. 603–611.
4) ROY, R., and F. A. MUMPTON (1958): Weathering Studies: 2. A Note on the Conversion of Phlogopite to Septechlorite. Ibid. Vol. 66, pp. 324–326.
5) GOTO, K. (1957): Colorimetric Determination of Aluminum in Industrial Waters Contating Iron. Chemistry and Industry, March 16, p. 329.
6) CORRENS, C. W., T. F. BARTH, and P. ESKOLA (1939): Die Entstehung der Gesteine. Julius Springer, Berlin.
7) OKAMOTO, G., T. OKURA, and K. GOTO (1957): Properties of Silica in Water. Geochimica et Cosmochimica Acta, Vol. 12, pp. 123–132.
8) GOTO, K., H. OCHI, and T. OKURA (1958): Determination of Aluminum in True Solution in the Presence of Colloidal Hydrated Alumina. Jour. Chemical Soc. Japan, Vol. 31, pp. 786–787.
9) HENDRICKS, S. D., and M. E. JEFFERSON (1939): Polymorphism of Micas with Optical Measurements. Am. Minera., Vol. 24, pp. 729–771.
10) BRINDLEY, G. W., and K. ROBINSON (1946): The Structure of Kaolinite. Min. Mag., Vol. 27, pp. 242–253.
11) HARADA, Z. (1936): Chemische Analysenresultate von Japanischen Mineralien. Jour. Fac. Sci. Hokkaido Univ., Ser. IV, Vol. III, Nos. 3–4, pp. 221–362.
12) ——— (1948): Chemical Analyses of Japanese Minerals (II). Ibid. Vol. VII, Nos. 1–2, pp. 143–210.
13) ——— (1954): Chemical Analyses of Japanese Minerals (III). Ibid. Vol. VIII, No. 4, pp. 289–348.
14) ——— (1959): Chemical Analyses of Japanese Minerals (IV). Ibid. Vol. X, No. 1, pp. 1–93.
15) BATES, T. F. (1958): Selected Electron Micrographs of Clays and Other Fine-grained Minerals. p. 7, The Pennsylvania State University.

(Nov. 1959)

Explanation of Plate I

Explanation of Plate I

Pseudomorphs of kaolinite after biotite. All figures are $\times 12$.

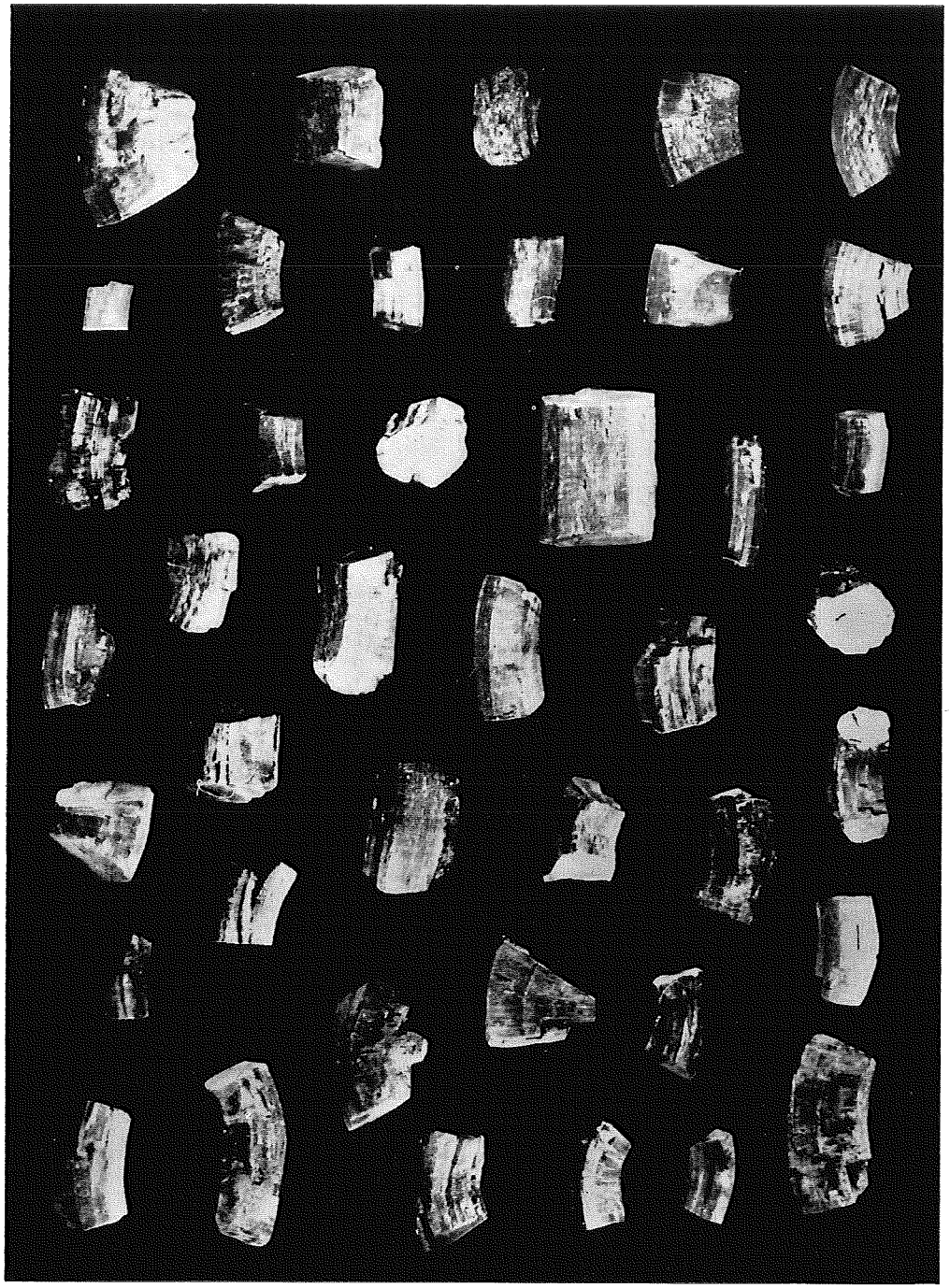

T. MITSUDA Photo.

Explanation of Plate II

Explanation of Plate II

Optical micrographs of kaolinite after biotite. B: unaltered biotite.
All figures are ×50.

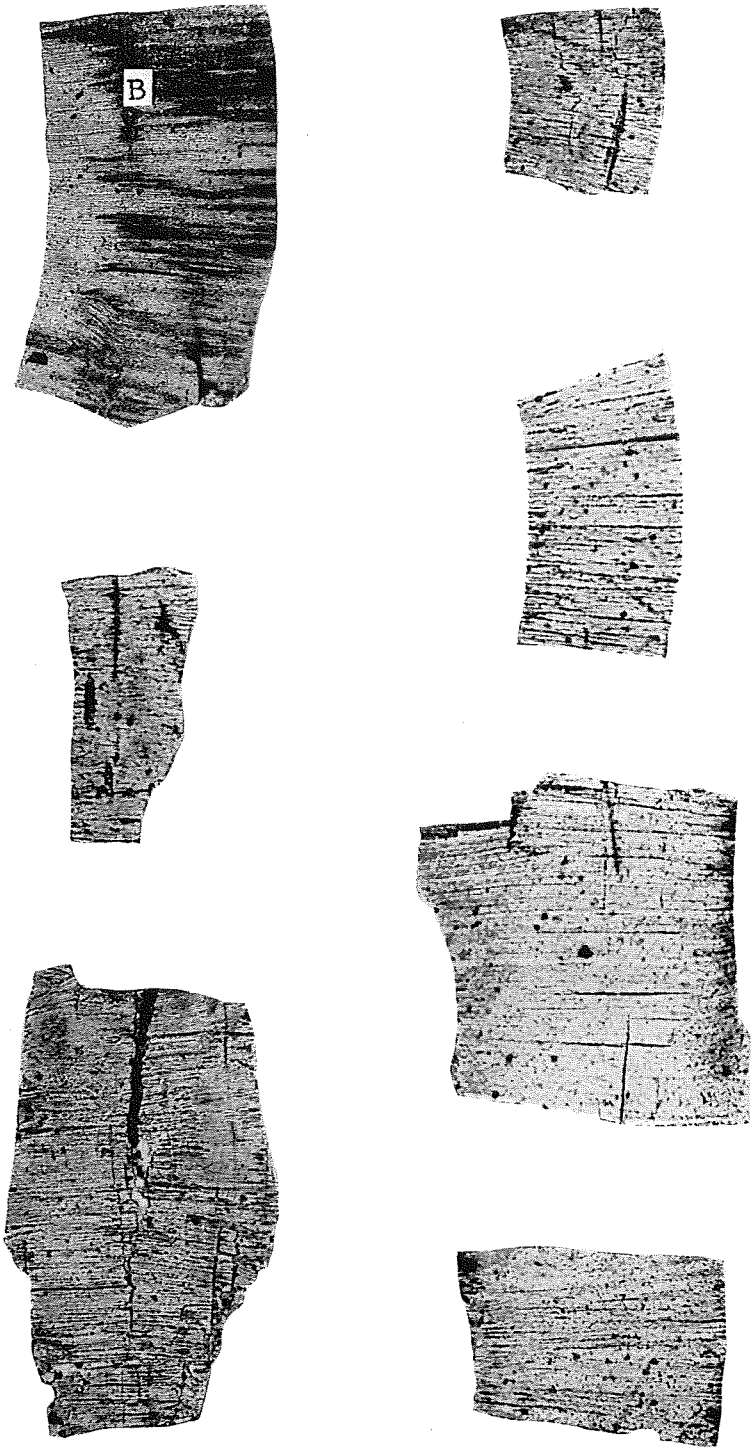

T. MITSUDA Photo.

Explanation of Plate III

Explanation of Plate III

Electron micrograph showing closed pores of cleavage surface of kaolinite after biotite.

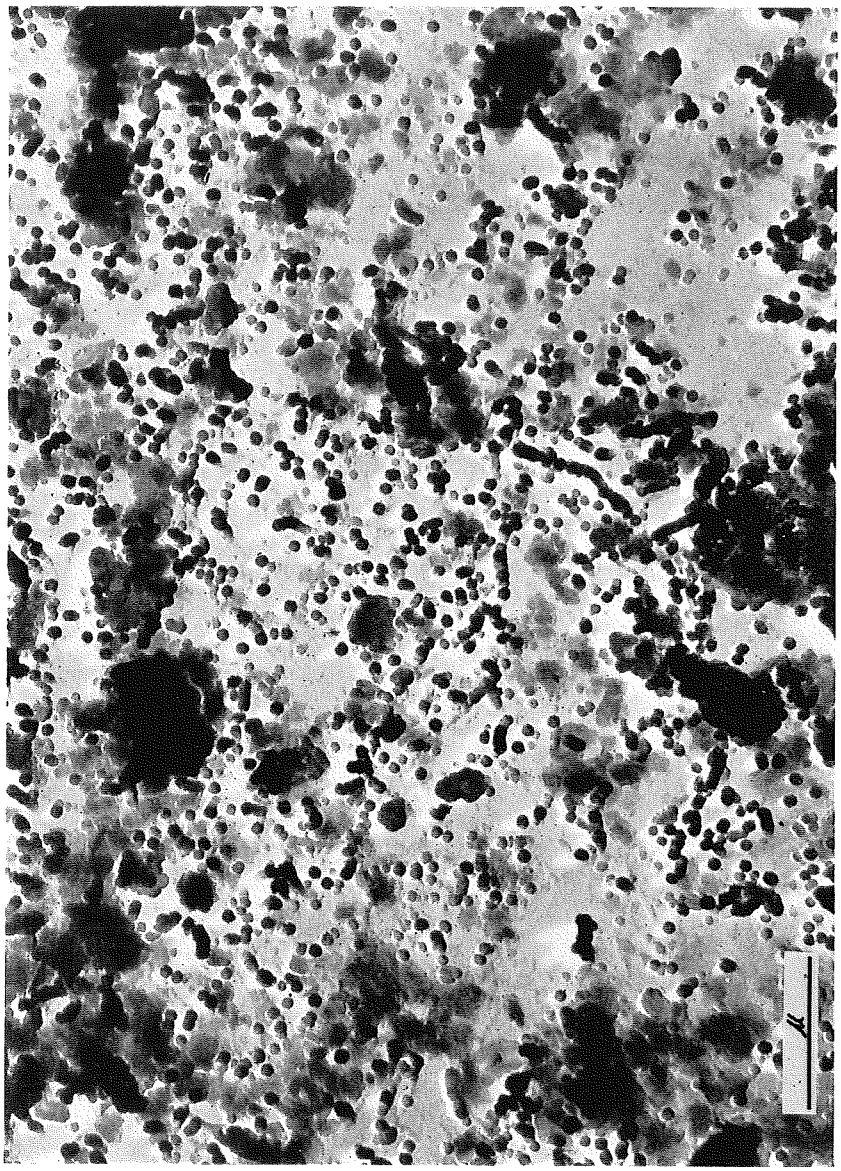

T. MITSUDA Photo.